Lesser, H. A., and Leon Lapidus, "The Time-Optimal Control of Discrete-Time Linear Systems with Bounded Control," *AIChE J.*, **12**, 143 (1966).
Luus, R., "Time-Optimal Control of State Constrained Linear Systems," *ibid.*, **19**, 1962 (1973).
———, "Optimal Control by Direct Search on Feedback Matrix," *Chem. Eng. Sci.*, **29**, 1013 (1974*a*).
———, "A Practical Approach to Time-Optimal Control of Nonlinear Systems," *Ind. Eng. Chem. Process Design Develop.*, **13**, 405 (1974*b*).
———, "Time-Optimal Control of Linear Systems," *Can. J. Chem. Eng.*, **52**, 98 (1974*c*).
———, and T. H. I. Jaakola, "Optimization by Direct Search and Systematic Reduction of the Size of Search Region," *AIChE J.*, **19**, 760 (1973).
Mayar, D. N., R. A. May, and R. Jackson, "The Time-Optimal Problem in Binary Batch Distillation With a Recycle Waste-Cut," *Chem. Eng. J.*, **1**, 15 (1970).
Nishida, N., A. Ichikawa, and E. Tazaki, "Optimal Design and Control in a class of Distributed Parameter Systems under Uncertainty—Application to Tubular Reactor With Catalyst Deactivation," *AIChE J.*, **18**, 561 (1972).
Paynter, J. D., and S. G. Bankoff, "Computational Methods in Process Optimization," *Can. J. Chem. Eng.*, **44**, 158 (1966).
Pearson, J. D., "Approximation Methods in Optimal Control," *J. Elect. Control*, **5**, 453 (1962).
Plant, J., and M. Athans, "An Iterative Technique for the Computation of Time Optimal Controls," *IFAC, London, England* (June, 1966).
Pontryagin, L. S., V. G. Boltayanskii, R. V. Gamkrelidze, and E. F. Mischemko, "The Mathematical Theory of Optimal Processes," Interscience, New York (1962).
Schlossmacher, E. J., "Deadbeat Control for a Class of Lumped Parameter Systems," *AIChE J.*, **19**, 409 (1973).
———, and Leon Lapidus, "The Suboptimal Control of Nonlinear Systems Using Lyapunov-Like Functions," *ibid.*, **17**, 1330 (1971).
Seinfeld, J. H., and Leon Lapidus, "Computational Aspects of Optimal Control of Distributed Parameter Systems," *Chem. Eng. Sci.*, **23**, 1461 (1968*a*).
———, "Singular Solutions in the Optimal Control of Lumped- and Distributed-Parameter Systems," *ibid.*, **23**, 1485 (1968*b*).
Siebenthal, C. D., and Rutherford Aris, "The Application of Pontryagin's Methods to the Control of a Stirred Tank," *ibid.*, **19**, 929 (1964).
Thomas, W. J., and R. M. Wood, "Use of the Maximum Principle to Calculate Optimum Catalyst Composition Profiles for Bifunctional Catalyst Systems Contained in Tubular Reactors," *ibid.*, **22**, 1607 (1967).
Tou, J. T., "Modern Control Theory," McGraw-Hill, New York (1964).
Weber, A. P. J., and Leon Lapidus, "Suboptimal Control of Constrained Nonlinear Systems," *AIChE J.*, **17**, 649 (1971).

Manuscript received November 26, 1975, and accepted January 29, 1976.

Trajectory Analysis of Deep-Bed Filtration with the Sphere-in-cell Porous Media Model

RAJAMANI RAJAGOPALAN
and
CHI TIEN
Department of Chemical Engineering and Materials Science
Syracuse University
Syracuse, New York 13210

This paper presents a model for the initial particle deposition in a deep-bed filter with a sphere-in-cell porous media model used. The analysis includes all the relevant mechanisms, and the results indicate that deposition occurs under favorable surface interactions. A semiempirical expression relating collection efficiency and operating parameters is presented.

SCOPE

The results reported in this study represent the continuing efforts of a long-range investigation whose objective is the development of a comprehensive theory of liquid filtration through granular beds. Such a theory of deep-bed filtration requires the selection of a mathematical and geometric model to characterize the bed for its hydrodynamic behavior and for its role as the collector of the particles in the suspension. The model chosen is then used to predict the dynamic behavior of the filtration process, that is, to predict the history of effluent quality and the corresponding change in the pressure drop across the filter. In this paper we employ the conceptually simple sphere-in-cell porous media model (Happel, 1958) to study the initial filtration efficiency with the help of the particle trajectory concept used in connection with other porous media models elsewhere (see Payatakes et al., 1974*a*, *b*, and *c*). The major objective of this work is to examine the use of this model for predicting initial collection rates in filters when the various filtration mechanisms such as sedimentation, interception, diffusion, and surface interactions act individually or collectively. Another important goal is to develop a semiempirical expression [Equation (27)] for the initial collection efficiency as a function of the pertinent process parameters. This is particularly desirable since such an expression would help avoid expensive computer work for future applications of this model.

CONCLUSIONS AND SIGNIFICANCE

The initial collection efficiency for filtration through granular beds is predicted within experimental error under a wide variety of conditions by the trajectory calculations made in this work with a sphere-in-cell porous media model. It is evident that an attractive surface force in the vicinity of the grains is required to permit filtration. Under such a condition, the collection rate depends on essentially four process parameters which characterize the ratio of the particle size to the grain size, the magnitude of the gravitational collection, the extent of the attractive

surface force, and the magnitude of Brownian diffusion. In order to avoid extensive and time-consuming computer usage for future use of this model, we have presented a semiempirical relation for the initial collection efficiency [Equation (27)] as a function of the above-mentioned parameters. Comparison of the results of this work with those of the constricted cell model proposed by Payatakes et al. (1973*a* and *b*; 1974*b* and *c*) indicates that it may be advantageous to combine this work and the constricted cell model for modeling the dynamics of deep-bed filtration.

Traditionally, theoretical investigations of deep-bed filtration have been limited mainly to the macroscopic study of the problem, which involves the solution of the conservation equation and the use of gross parameters to characterize the bed behavior (for example, see Ives, 1971). The introduction of the particle trajectory concept by Yao (1968), then used primarily in aerosol filtration, for the study of particle deposition in water filtration has opened up a new phase in the theoretical studies. Nevertheless, the trajectory analysis alone cannot provide the complete answer to the problem, since a theoretical analysis of deep-bed filtration consists of at least two important steps:

1. The selection of an appropriate porous media model to characterize the filter bed for its fluid mechanical behavior and its role as an assembly of particle collectors.
2. The choice of a suitable theoretical technique to estimate the rate of particle retention and the change of the structure of the filter media due to particle deposition. From the knowledge of the structural change, one can, in principle, predict the increase in resistance to flow due to particle retention.

The first requirement of the second step is served by the particle trajectory concept. For the first step, a number of choices are available. Porous media models including a simple capillaric model, spherical collector models, and a rather complicated constricted tube model have all been used as a basis of study. Generaly speaking, the study of particle deposition (or filtration rate) is comparatively simple as compared to the estimation of the pressure drop increase, and the search for a satisfactory porous media model for the study of the complete dynamic behavior of deep-bed filters has not been entirely successful up to the present time. Among the various models tested so far, the constricted tube model is of potential significance since its structure is more amenable to reflect the consequences brought about by particle deposition. Furthermore, trajectory calculations based on this model (Payatakes et al., 1974*b* and *c*) were found to give reasonably good agreements with experimental data. The difficulty with the use of the constricted tube model is the excessive computation required, since one has to solve both the pertinent flow equation and the trajectory equation numerically, whereas the other models require numerical approach only for the trajectory equation.

As a possible way to circumvent this difficulty, it is conceivable that one may employ a simpler model for the study of particle deposition and the constricted tube model for the study of change of resistance (that is, pressure drop increase). The premise of this approach, of course, rests on the assumption that the model adopted for predicting particle deposition will give the same degree of accuracy as obtained with the constricted tube model. In the past, the authors have examined the capillaric, Brinkman, and single-sphere models (Payatakes et al., 1974*a*; Rajagopalan, 1974). More recently, investigations using the sphere-in-cell (Happel's) model have been made, the results of which are reported in this paper. It should be noted that trajectory calculations purportedly based on Happel's model have been reported in the literature (FitzPatrick, 1972; Spielman and FitzPatrick, 1973). However, the numerical results of these studies were obtained with approximations both in the trajectory equation and the flow field. Furthermore, the numerical integration of the trajectory equation was often carried out beyond the domain of definition of the model. A more detailed discussion of the differences between the present work and these earlier studies is given in later sections.

The present work is concerned with the deposition of particles in a deep-bed filter. The filter bed is represented by the Happel's sphere-in-cell model, and the deposition is determined from the integration of the trajectory equation which takes into account all the major forces with the exception of that due to Brownian motion. The influence of Brownian motion is separately computed by using Cookson's (1970) work. Based on the numerical results, simple empirical expressions relating the initial collection efficiency with the various relevant process parameters have been developed. The availability of these empirical expressions makes it possible to apply the results of the trajectory calculations without extensive numerical calculations.

THE TRAJECTORY CONCEPT

When a liquid suspension flows through a filter bed, the particulate matters deposit onto the surfaces of the grains of the filter medium. Such deposition is caused by various mechanisms, the four most important among them being diffusion, interception, gravitational collection, and collection due to surface forces. Of these, diffusion dominates only for the submicron particles; thus, for the larger particles one can, at least theoretically, follow the particle trajectories to compute what fraction of the particulate matter is collected by the grains. This, however, requires an appropriate description of the filter bed in terms of an assembly of collectors and of the flow field around (or through) these collectors. The trajectories themselves are obtained by integrating the trajectory equation, which in turn is obtained by writing a force balance on the suspended particle. If the trajectory of a particle intercepts the collector, then that particle is assumed to be captured.

However, it is not necessary to follow each particle to determine if it is collected or not. In actual computation, the degree of particle collection is expressed in terms of the collection efficiency η, which is determined through the location of the so-called limiting or critical trajectory. The limiting trajectory is defined to be the trajectory that separates the trajectories that intercept the collector from those that do not* (see Figure 1). This definition simplifies the computation of the amount of particles collected, and the initial collection efficiency η is then given by the ratio of amount of particles collected to that approaching the collector.

* If the particle inertia is not considered in the force balance, the trajectories do not intercept each other.

HAPPEL'S SPHERE-IN-CELL POROUS MEDIA MODEL

In Happel's original formulation, which was concerned primarily with the estimation of the pressure drop across a packed bed, the granular bed (such as a filter) is assumed to be comprised of spherical collectors, each of which is encircled by a spherical liquid envelope that is taken to be frictionless along its outer surface (Happel, 1958). The diameter of the envelope is so chosen that the porosity of the combined entity (namely, the spherical grain and the liquid envelope) is equal to the macroscopic porosity of the granular bed. The velocity external to the spherical collector is obtained under the condition that the fluid is stationary as the solid sphere moves upward with a velocity U. The equation of motion for the creeping flow is solved with the following boundary conditions: the radial velocity at the outer surface of the liquid shell is zero, the tangential stress at the outer surface is zero, and the no-slip condition holds at the solid-liquid boundary.

Under these conditions, the stream function for the region $a_s \leq r \leq b$ is given by

$$\left.\begin{aligned} \psi = (U/2)\sin^2\theta\, a_s^2[(K_1/r^*) \\ + K_2 r^* + K_3 r^{*2} + K_4 r^{*4}] \end{aligned}\right\} \quad (1)$$

where

$$\left.\begin{aligned} r^* &= r/a_s \\ K_1 &= 1/w \\ K_2 &= (3 + 2p^5)/w \\ K_3 &= p(3 + 2p^5)/w \\ K_4 &= -p^5/w \\ w &= 2 - 3p + 3p^5 - 2p^6 \end{aligned}\right\}$$

and

$$p = (1 - \epsilon)^{1/3} = a_s/b$$

In Equation (1), ϵ is the porosity of the bed, a_s is the radius of the spherical collector, and b is the outer radius of the spherical liquid envelope. The coordinate system is shown in Figure 1.

The solution given in Equation (1) is transformed to the case corresponding to the situation in a filter bed (where the grains are stationary and the liquid is moving down) by superimposing a uniform flow field given by $\psi = 1/2\ Ur^2 \sin^2\theta$. Notice that this is equivalent to imposing a uniform flow field with a downward velocity U. The resulting stream function for $a_s \leq r \leq b$ is

$$\psi = (U/2)\, a_s^2 \sin^2\theta\, [(K_1/r^*) + K_2 r^* + K_3' r^{*2} + K_4 r^{*4}] \quad (2)$$

where

$$K_3' = (2 + 3p^5)/w$$

Equation (2) is valid only over the spherical envelope (that is, $a_s \leq r \leq b$), and it is convenient to view the sphere-in-cell model as a mapping of the entire filter bed inside a sphere of radius b. The total volumetric flow into and out of this configuration is given by $\pi b^2 U$.

PROBLEM STATEMENT AND DESCRIPTION OF THE METHOD OF SOLUTION

The trajectory equation that forms the basis of the present paper is simply a consequence of the dynamic equilibrium of the suspended particle under the action of various forces. The forces considered in the present analysis are due to gravity, buoyancy of the particle, fluid motion (convection), and the surface interactions (London attraction and double-layer repulsion or attraction). The notable exclusion in the force balance is the force due to molecular bombardment of the liquid molecules on the particle. Such molecular bombardments result in the so-called Brownian diffusion and are negligible for suspended particles of diameter greater than about 1 μm.

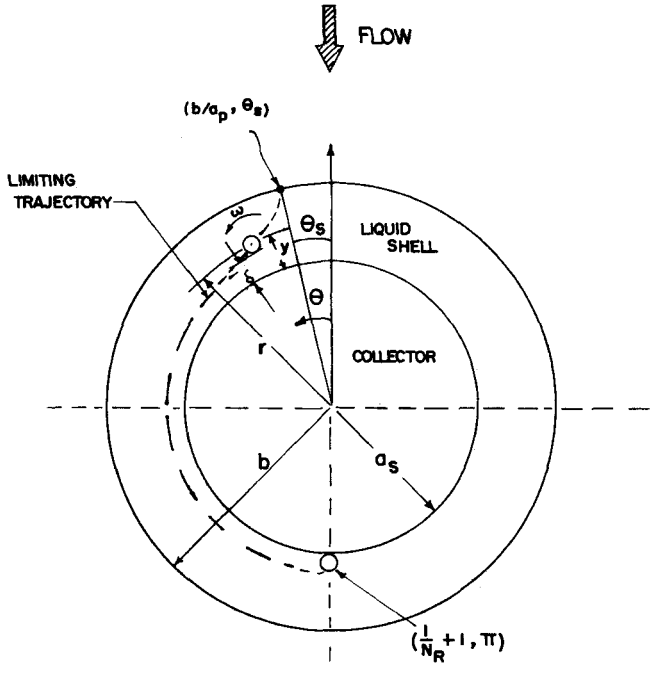

Fig. 1. Happel's sphere-in-cell porous media model.

The formulation of the trajectory equation is based on the assumption that the particle concentration is sufficiently low so that the motion of any given particle does not interfere with those of the others. We further assume that the motion is axisymmetric. (This is a consequence of the axisymmetry of the flow field of the liquid.)

Under the condition of dynamic equilibrium of the suspended particle, one has

$$\left.\begin{aligned} f^G + f^{Lo} + f^{DL} + f^D + f^I = 0 \\ \text{and} \\ t^G + t^{Lo} + t^{DL} + t^D + t^I = 0 \end{aligned}\right\} \quad (3)$$

where **f** and **t** are the forces and torques acting on the particles, and the superscripts G, Lo, DL, D, and I stand for gravity, London attraction, double-layer interaction, drag, and inertia, respectively. Such a force balance has already been presented by Payatakes et al. (1974*a*) in connection with the capillaric and Brinkman models. Hence, we present here only the final equations. However, for the sake of convenience and easy reference, the various force components considered in the formulation of the trajectory equations are presented in Table 1.

The velocity of the liquid around the collector is obtained from Equation (2) and is given by

$$\mathbf{v} = -\left(\frac{1}{r\sin\theta}\frac{\partial\psi}{r\partial\theta}\right)\mathbf{e}_r + \left(\frac{1}{r\sin\theta}\frac{\partial\psi}{\partial r}\right)\mathbf{e}_\theta \quad (4)$$

However, the drag correction factors that appear in Table 1 require that the fluid velocity be specified in the following form:

$$\mathbf{v} = -Ay^2\mathbf{e}_r + (By + Dy^2)\mathbf{e}_\theta \quad (5)$$

For this reason, the coefficients A, B, and D have been obtained for trajectory calculations by approximating Equation (4) in the required form over segments of the Happel shell (see, for instance, Rajagopalan, 1974).

The force and torque balance described above provide the following expressions for the r and θ directed particle velocities:

TABLE 1. FORCES AND TORQUES ACTING ON THE SUSPENDED PARTICLES

I. Inertial force and torque

$$\mathbf{f}^I = m\frac{D\mathbf{u}}{Dt}$$

where

$$\frac{D}{Dt} = \left(\frac{\partial}{\partial t} + \mathbf{u}\cdot\nabla\right)$$

$$\mathbf{t}^I = \mathbf{0}$$

II. Gravitational force and torque

$$\mathbf{f}^G = (4/3)\pi a_p^3(\rho_p - \rho_f)\mathbf{g}$$

$$= (4/3)\pi a_p^3(\rho_p - \rho_f)g[-\cos\theta\,\mathbf{e}_r + \sin\theta\,\mathbf{e}_\theta]$$

$$\mathbf{t}^G = \mathbf{0}$$

$$g = |\mathbf{g}|$$

III. Surface force and torque

a) Molecular dispersion force and torque (London force and torque)

$$\mathbf{f}^{Lo} = [-2H\alpha(\delta; a_p, \lambda_e)\, a_p^3/3\delta^2(2a_p + \delta)^2]\mathbf{e}_r$$

where $\alpha(\delta; a_p, \lambda_e)$ is the retardation correction factor

$$\mathbf{t}^{Lo} = \mathbf{0}$$

Double-layer interaction force and torque*

$$\mathbf{f}^{DL} = \{[\upsilon a_p\kappa(\zeta_c^2 + \zeta_p^2)/2] \times [(2\zeta_c\zeta_p/(\zeta_c^2 + \zeta_p^2)) - e^{-\kappa\delta}]\,[e^{-\kappa\delta}/(1 - e^{-2\kappa\delta})]\}\,\mathbf{e}_r$$

$$\mathbf{t}^{DL} = \mathbf{0}$$

IV. Drag forces and torques†**

(a) Due to the translation of the particles

$$(\mathbf{f}^D)^t = -6\pi\mu a_p[\mathbf{u}_r f_r^t(\delta^+)\mathbf{e}_r + \mathbf{u}_\theta f_\theta^t(\delta^+)\mathbf{e}_\theta]$$

$$(\mathbf{t}^D)^t = 8\pi\mu a_p^2\,\mathbf{u}_\theta\, g_\phi^t(\delta^+)\mathbf{e}_\phi$$

(Brenner, 1961; Goren and O'Neill, 1971; O'Neill, 1964)

b) Due to the rotation of the particle

$$(\mathbf{f}^D)^r = 6\pi\mu a_p^2\,\omega f_\theta^r(\delta^+)\mathbf{e}_\theta$$

$$(\mathbf{t}^D)^r = -8\pi\mu a_p^3\,\omega g_\phi^r(\delta^+)\mathbf{e}_\phi$$

where

$$\omega = |\boldsymbol{\omega}|$$

(Goldman, Cox, and Brenner, 1967*a*)

c) Due to the fluid velocity in the presence of the stationary particle:

$$(\mathbf{f}^D)^m = 6\pi\mu a_p\{-A\,y^2 f_r^m(\delta^+)\mathbf{e}_r + [B\,y\,f^m{}_{1\theta}(\delta^+) + D\,y^2 f^m{}_{2\theta}(\delta^+)]\,\mathbf{e}_\theta\}$$

$$(\mathbf{t}^D)^m = 8\pi\mu a_p^3\,[B\,g^m{}_{1\phi}(\delta^+) + D\,y g^m{}_{2\phi}(\delta^+)]\mathbf{e}_\phi$$

(Goren and O'Neill, 1971; Goldman, Cox, and Brenner, 1967*b*)

* The potentials ζ_c and ζ_p in the expression for $\mathbf{f}^{DL}$ are actually the so-called surface potentials (see, for instance, Hogg, Healy, and Fuerstenau (1966)). But it is a common practice to equate them to the corresponding zeta potentials. In computing the force due to the double-layer interaction, the unit of the zeta potentials should be in electrostatic units.

† See Rajagopalan (1974) for the tabulation of all correction factors.

** The references following the entries may be consulted for further details.

$$\mathbf{u}_r^* = \frac{1}{U}\frac{dr}{dt} = \frac{1}{f_r^t}\{-A^+(1+\delta^+)^2 f_r^m - N_G\cos\theta + N_{E1}[N_{E2} - e^{-N_{DL}\delta^+}] \times [e^{-N_{DL}\delta^+}/(1 - e^{-2N_{DL}\delta^+})] - [N_{Lo}\alpha(\delta^+; N_{Rtd})/(\delta^{+2})(2+\delta^+)^2]\} \quad (6)$$

$$\mathbf{u}_\theta^* = \frac{r}{U}\frac{d\theta}{dt} = \frac{1}{s_1}\{B^+ s_2 + D^+(1+\delta^+)s_3 + N_G\sin\theta\} \quad (7)$$

In the above equations, N_G, N_{E1}, N_{E2}, N_{DL}, N_{Lo}, and N_{Rtd} are dimensionless numbers that characterize the various forces acting on the particle. The wall-effect correction factors introduced by the presence of the collector wall (see Table 1) also appear in the above equations in certain combinations (namely, s_1, s_2, s_3). The trajectory equation for the suspended particle is obtained by eliminating the time differential from Equations (6) and (7):

$$\frac{d\delta^+}{d\theta} = \left(\frac{1}{N_R} + 1 + \delta^+\right) \times \frac{\text{right-hand side of Equation (6)}}{\text{right-hand side of Equation (7)}} \quad (8)$$

where the parameter N_R is given by (a_p/a_s).

Equation (8) is a first-order differential equation and does not have a closed-form solution. However, the numerical technique required is rather straightforward. In this work, Equation (8) has been solved by using the fourth-order Runge-Kutta method.

The solution of Equation (8) requires an initial condition, namely, starting position of the particle whose trajectory is desired. Since we are interested in only those particles that are captured, it is convenient to start from the surface of the collector. For example, use of a condition such as

$$\mathbf{r}_o{}^+ = \left(\frac{1}{N_R} + 1, \theta_o\right) \quad (9)$$

in the integration scheme would result in the trajectory of a particle that eventually intercepts the collector at the position $\mathbf{r}_o{}^+$. Notice that Equation (9) has incorporated collection due to interception by accounting for the finite size of the particle [that is, $r_o{}^+ \neq a_s/a_p$, but rather $(a_s + a_p)/a_p$]. However, since we are interested in the limiting trajectory, the initial condition of interest would be

$$\mathbf{r}_o{}^+ = \left(\frac{1}{N_R} + 1, \pi\right) \quad (10)$$

The termination point of integration in the case of the sphere-in-cell model is simply

$$r^+ = b/a_p \quad (11)$$

where b is the outer radius of the spherical shell surrounding the collector.

The solution of Equations (8) and (10) is thus used to obtain the starting position of the limiting trajectory at the Happel shell. Denoting this by

$$\mathbf{r}_s{}^+ = (b/a_p, \theta_s) \quad (12)^*$$

we note that the volumetric flow of suspension through the circular cross section enclosed by the limiting trajectory is given by

$$(\text{volume/unit time}) = \pi(b^2\sin^2\theta_s)\,U \quad (13)$$

Since the total volumetric flow rate through the shell is given by $\pi b^2 U$, the initial collection efficiency η is given by

$$\eta = (\pi b^2 U\sin^2\theta_s\, C_o)/(\pi b^2 U\, C_o) = \sin^2\theta_s \quad (14)$$

* Notice that the purpose of the integration is the determination of θ_s.

where C_o is the number of particles per unit volume of the suspension at the entrance to the shell. In the past, the collection efficiency has been expressed as a multiple of the efficiency due to interception alone (denoted by η_I), which can be obtained from the expression for the stream function [that is, Equation (2)] as

$$\eta_I = \left\{ 2\pi\psi \,\middle|_{r^+ = \left(\frac{1}{N_R} + 1, \pi/2\right)} \div \pi b^2 U \right\} \approx 1.5\, N_R{}^2 \left(\frac{a_s}{b}\right)^2 \left[\frac{2(1-p^5)}{w}\right] \quad (15)$$

$$= 1.5\, N_R{}^2 \left(\frac{a_s}{b}\right)^2 A_s \quad (16)^*$$

In the case of filter beds, $\epsilon \approx 0.39$, and hence

$$(a_s/b)^2 \approx 1/1.4 \quad (17)$$

Equations (14) and (15) imply that η and η_I are always less than (or, at most, equal to) 1. As pointed out earlier, the trajectory equation for the particle has been formulated by excluding the Brownian movement of the particles. Consideration of the random molecular fluctuations that cause this motion would make the resulting equation stochastic in nature. Although, technically, the solution would still be known as the trajectory of the particle, such a solution is not deterministic but is characterized by probability distributions. The appropriate setting for this analysis would then be the theory of diffusion processes as shown by Rajagopalan (1974). For our purpose here, it is expedient and sufficient to treat the Brownian motion separately. That such an analysis is adequate enough for the consideration of diffusion in filter beds has been shown by Yao (1968) and more recently by Prieve and Ruckenstein (1974).

Cookson (1970) used the sphere-in-cell model for calculating the rate of diffusional mass transfer in packed beds. It follows from his analysis that the efficiency of collection due to diffusion alone is given by

$$\eta_{\text{Diff}} \cong 4 \left[\frac{2(1-p^5)}{w}\right]^{1/3} N_{Pe}{}^{-2/3} = 4A_s{}^{1/3} N_{Pe}{}^{-2/3} \quad (18)$$

where N_{Pe} is the Peclet number defined by

$$N_{Pe} = \frac{d_s U}{D_{BM}} \quad (19)$$

D_{BM} in Equation (19) is the diffusion coefficient of the suspended particle given by

$$D_{BM} = kT/6\pi\mu a_p \quad (20)$$

where k is the Boltzmann constant, T is the absolute temperature of the suspension, and μ is the viscosity of the suspension.

In interpreting filtration data, the collection results often are presented in terms of the so-called filter coefficient λ defined by

$$\lambda = -\frac{3(1-\epsilon)}{2d_s} \ln(1-\eta) \quad (21)$$

However, since η is often very low, the following equation for λ is a good approximation for Equation (21):

$$\lambda \approx \frac{3(1-\epsilon)}{2d_s}\eta \quad (22)$$

* This expression is obtained by excluding all the other mechanisms and the wall effect on the drag force.

NUMERICAL RESULTS

By using the analysis outlined in the previous section, computer runs were made to solve the trajectory Equation (8) for typical parameters (N_G, N_R, and N_{Lo}) encountered in deep-bed filtration. The results are shown in Figures 2 to 5.

The theoretical calculations can be grouped under two major headings: collection under favorable surface conditions (that is, attractive surface forces), and collection under unfavorable surface conditions (that is, repulsive surface interaction in the vicinity of the collector). Rajagopalan (1974) and Payatakes et al. (1974*b* and *c*) have already shown that the theory predicts negligible or no collection when a repulsion barrier exists in the neighborhood of the collector surface. Thus, it is sufficient to consider the first of the above two cases. Figure 2 presents the calculated values of η as a function of N_R and N_G at constant N_{Lo} ($= 1.45 \times 10^{-5}$). In deep-bed filtration, N_G varies from exceedingly small values up to $\sim 10^{-1}$, and N_R varies from about 10^{-4} to 10^{-1}. The broken lines in Figure 2 correspond to the omission of the viscous interaction introduced by the collector wall. For $N_G = 0$, η is a linear function of $N_R{}^2$. This follows from the fact that the collection is entirely due to interception, which is given by Equation (16), and hence the second-power dependence on N_R. For $N_G > 0$, η increases monotonically with N_R. For low values of N_R, the lines tend to an asymptotically constant value due to the fact that interception is no longer important, and the only other mechanism, sedimentation, dominates. In fact, the asymptotic values are approximately $N_G(a_s/b)^2$, thereby indicating that the efficiency due to gravity alone is approximately

$$\eta_G \approx N_G \left(\frac{a_s}{b}\right)^2 \quad (23)$$

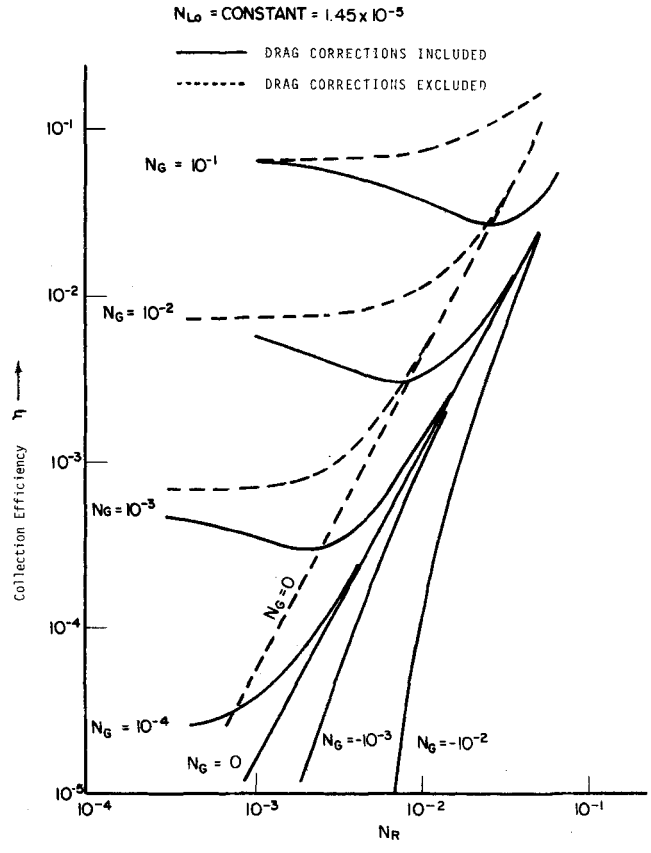

Fig. 2. Theoretical initial collection efficiency as a function of N_R and N_G (N_{Lo} = constant).

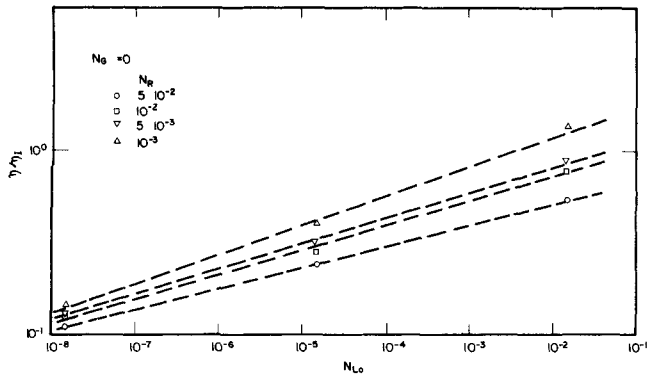

Fig. 3. (η/η_I) vs. N_{Lo} at constant N_R ($N_G = 0$).

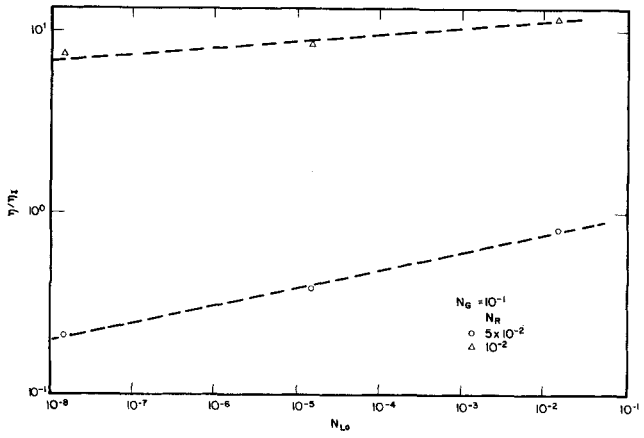

Fig. 4. (η/η_I) vs. N_{Lo} at constant N_R for large N_G ($N_G = 10^{-1}$).

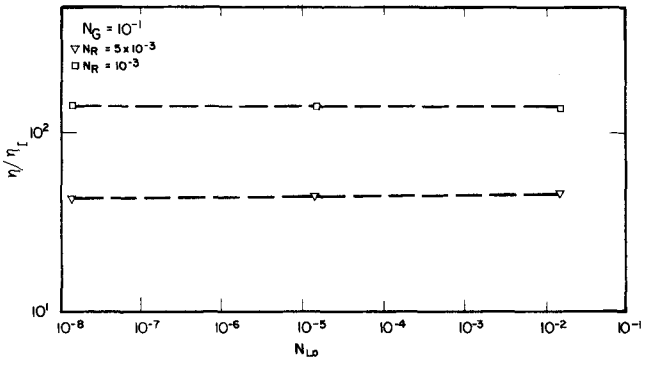

Fig. 5. (η/η_I) vs. N_{Lo} at constant N_R for large N_G ($N_G = 10^{-1}$).

Indeed, it turns out that when wall corrections are ignored, the initial collection efficiency η is simply

$$\eta \approx \eta_G + \eta_I \tag{24}$$

that is, the broken lines of Figure 2 are given by Equation (24). This means that interception and gravity act almost independently. This result is rather interesting, since similar results have been shown to hold for the case of the single collector model by Rajagopalan (1974) and for the case of the Brinkman model by Rajagopalan and Tien (unpublished).

Inclusion of drag corrections in the trajectory analysis (to account for deviation from Stokes' law for drag force on the particle due to the presence of the collector surface) would decrease the rate of collection. This is due to the fact that the increased viscous resistance in the neighborhood of the collector surface hinders the particle from moving closer to the collector. The solid lines in Figure 2 indeed show that this is the case. For instance, at $N_G = 0$ the efficiency is still linear with respect to N_R but lower than the previous case. It should be noted, however, that the collection would have been zero in this case were the London attraction not included. In the absence of this attractive force, the particle would have been unable to make contact with the collector because of the lack of any aid to overcome the viscous barrier.

For $N_G > 0$, three regions can be recognized. For very low N_R ($\lesssim 10^{-3}$), sedimentation dominates so heavily that viscous interaction hardly diminishes collection. The efficiency in this case tends to a constant value [equal to η_G of Equation (23)]. For very large values of N_R ($N_R \to 10^{-1}$), interception starts dominating (aided by London attraction), and the influence of gravity decreases. Between these two extremes, the collection efficiency displays a minimum. The physical significance of this behavior is rather straightforward but nevertheless is of considerable importance. It is simply a consequence of the fact that as the ratio of the particle size to the collector size increases, the significance of the viscous resistance is shadowed by the increase in collection due to interception caused by the presence of the neighboring grains. [In fact, for $N_R \approx 10^{-1}$, interception is so significant that even increases in N_G (sedimentation) at constant N_R introduce imperceptible changes in the collection efficiency.] Indeed, Rajagopalan (1974) has shown that such a behavior is absent in the case of the single collector models, where η shows a monotonic decrease as N_R increases, since the single collector models by their very nature exclude the presence of neighboring grains. Consequently, we believe that the behavior shown in Figure 2 is a desirable (and probably essential) feature of any model for the deep-bed filter, for it may explain the increase in the filter coefficient during the initial period of filtration reported by many investigators (see, for instance, Weber, 1972). In this connection, it is instructive to examine the predictions of the constricted cell model proposed by Payatakes et al. (1974*c*), since their model is also designed to include the effects of the other grains in the bed. A reexamination indeed reveals that the minimum in η vs. N_R reported by Payatakes et al. (1974*c*) is caused by the increase in interception for high values of N_R. [Payatakes et al. (1974*c*) and Payatakes (1973) claim that the minimum observed is a consequence of the changes in "the relative magnitude of the forces for various particle diameter values with the other dimensionless parameters adjusted so that the rest of the dimensionless groups remain constant." This explanation, however, is inaccurate since, firstly, interception is not a force, and, secondly, the restriction of the other parameters to constant values implies that in effect all the forces are held constant. In fact, that is the basis of any case study involving dimensionless groups. Furthermore, there is no need to change the particle size to vary N_R. Instead, one can change the collector diameter without affecting any other dimensionless group, that is, leaving all forces unaffected.]

Figures 3, 4, and 5 show the influence of the London group N_{Lo} on η at constant N_R and N_G. For $N_G = 0$ (Figure 3), ln (η/η_I) is almost a linear function of ln N_{Lo} at constant N_R. As shown in Figures 4 and 5, this seems to be true in the case of high values of N_G also, except that in this case at low values of N_R, (η/η_I) is practically constant (Figure 5). In fact, even for large N_R, the rate of increase of (η/η_I) with respect to N_{Lo} (Figure 4) is almost the same as it is for the same values of N_R at $N_G = 0$ (Figure 3). This suggests that at constant N_R, the dependence of (η/η_I) on N_{Lo} at nonzero N_G may be approximately the same as its dependence on N_{Lo} at $N_G = 0$. Also, the approximate linearity of ln (η/η_I) vs. ln N_{Lo}

TABLE 2. LIST OF DIFFERENCES BETWEEN THE PRESENT WORK AND THAT OF SPIELMAN AND FITZPATRICK

	Spielman and Fitzpatrick model	Present work
Forces excluded	Retardation of London attraction and gravity and buoyancy in θ direction	None
Form of radial fluid velocity	$-Ay^2$; A is not a function of r	$-Ay^2$, A depends on r
Form of angular fluid velocity	Dy^2; D is not a function of r	$By + Dy^2$; B and D are dependent on r
Form of angular particle velocity	$a_s \frac{d\theta}{dt}$	$r \frac{d\theta}{dt}$
Trajectory equation	Function of $N_{Ad,s}$ and $N_{Gr,s}$ Not an explicit function of N_R	Function of N_G, N_R, N_{Lo}, N_{Rtd}, N_{E1}, N_{E2}, and N_{DL}
Point of termination of the trajectory	100 a_p or greater Corresponds to (in some cases) 12 a_s or about 60 times shell thickness	The outer radius of the Happel cell Never exceeds the Happel shell

indicates that (η/η_I) can be expressed as a power of N_{Lo}.

In short, we are interested in an approximate, yet sufficiently accurate, expression for (η/η_I), since this would make extensive computer calculations unnecessary for further use of this model. To obtain such an approximate expression, figures similar to Figures 3, 4, and 5 were constructed by keeping two of the dimensionless groups constant and varying the third. The resulting expression is given by

$$\eta \approx \eta_I \left[\frac{2}{3} N_{Lo}^{1/8} N_R^{-1/8} + 2.25 \times 10^{-3} N_G^{1.2} N_R^{-2.4} \right];$$

$$N_R < \frac{b}{a_s} - 1 \approx 0.18^* \quad (25)$$

The first expression on the right-hand side of Equation (25) is for $N_G = 0$, and both the first and the second terms together represent the case $N_G > 0$. Notice that η cannot be expressed in terms of just one expression involving powers of N_R, N_G, and N_{Lo}, since that would mean that $\eta = 0$ for $N_G = 0$, thereby ignoring the effect of interception and London attraction at $N_G = 0$.

Also, notice that Equation (25) predicts nonzero values for η when N_G and $N_R \neq 0$ but $N_{Lo} = 0$. As mentioned earlier, exclusion of London attraction would imply that $\eta = 0$ if viscous corrections are to be included in the trajectory calculations. This discrepancy in Equation (25) is the result of the assumption that the dependence of η on N_{Lo} for nonzero N_G is entirely due to its dependence on N_{Lo} for $N_G = 0$. This assumption has been made to simplify the determination of Equation (25). However, this assumption is by no means a restriction, since in practice N_{Lo} can never be zero.

If η_I from Equation (16) and $(a_s/b)^2$ from Equation (17) are substituted into Equation (25), one obtains

$$\eta \approx 0.72 A_s N_{Lo}^{1/8} N_R^{15/8} + 2.4 \times 10^{-3} A_s N_G^{1.2} N_R^{-0.4};$$

$$N_R \lesssim 0.18 \quad (26)$$

The contribution of diffusion may also be added to Equation (26), thus giving for the total collection efficiency

$$\eta \approx 0.72 A_s N_{Lo}^{1/8} N_R^{15/8} + 2.4 \times 10^{-3} A_s N_G^{1.2} N_R^{-0.4} + 4 A_s^{1/3} N_{Pe}^{-2/3}; \quad N_R \lesssim 0.18 \quad (27)$$

Equation (27) thus gives an approximate closed-form solution for the initial collection efficiency in deep-bed filters by using Happel's model.

COMPARISON WITH OTHER THEORETICAL INVESTIGATIONS

As mentioned earlier, FitzPatrick (1972) and Spielman and FitzPatrick (1973) have presented trajectory calculations for particle deposition in deep-bed filters based on Happel's model. There are, however, significant differences between the present work and the earlier study, as shown in Table 2. These differences arise mainly from the approximations made in the flow field and in the trajectory equation used in FitzPatrick (1972). The major differences in FitzPatrick (1972) are:

1. Use of a second-order approximation for the stream function throughout the entire calculation.
2. Extension of the region of integration considerably beyond the domain of the Happel cell.
3. Use of an approximate expression for the radial velocity of the particle (that is, $a_s\, d\theta/dt$ instead of $r d\theta/dt$).*

The second-order approximation for the stream function is given by

$$\psi = \frac{3}{4} A_s U (r - a_s)^2 \sin^2 \theta \quad (28)$$

A comparison of the velocity components derived from the above expression with those based on Happel's model is shown in Figure 6. Notice that the velocity components are not defined for $r \gtrsim 1.178\ a_s$ in the case of Happel's model. This value of r corresponds to the outer boundary of the Happel cell. Also notice that the velocities based on Equation (28) are vastly different from Happel's solution even within the liquid shell. When these are extended beyond the cell boundary, the values diverge and are around 10^3 times the approach velocity at a distance of about 50 times the shell thickness!

In FitzPatrick's calculations the termination point of the trajectory equation has been specified to be 100 a_p or greater (see Appendix B of FitzPatrick, 1972), and thus consideration of the region beyond the Happel shell is unavoidable in many cases. A case in point is the set of calculations corresponding to the first thirteen runs of FitzPatrick (1972). For this set, $d_s = 180\ \mu$m and $d_p =$

* Notice, however, that the expressions used in the trajectory equation for the surface interactions and the wall corrections will be, at the most, approximate for $N_R \geq 0.18$. This is due to the fact that these expressions are derived under the assumption that the particle and the collector can be treated as a sphere and a plane, respectively, when the distance of separation between them is small. This restriction also applies to the constricted cell model of Payatakes et al. (1973*a* and *b*) and to the other models mentioned in the text.

* If the integration is terminated very close to the collector surface, this approximation is accurate enough. However, because of difference No. 2 above, the approximate radial velocity introduces considerable deviation.

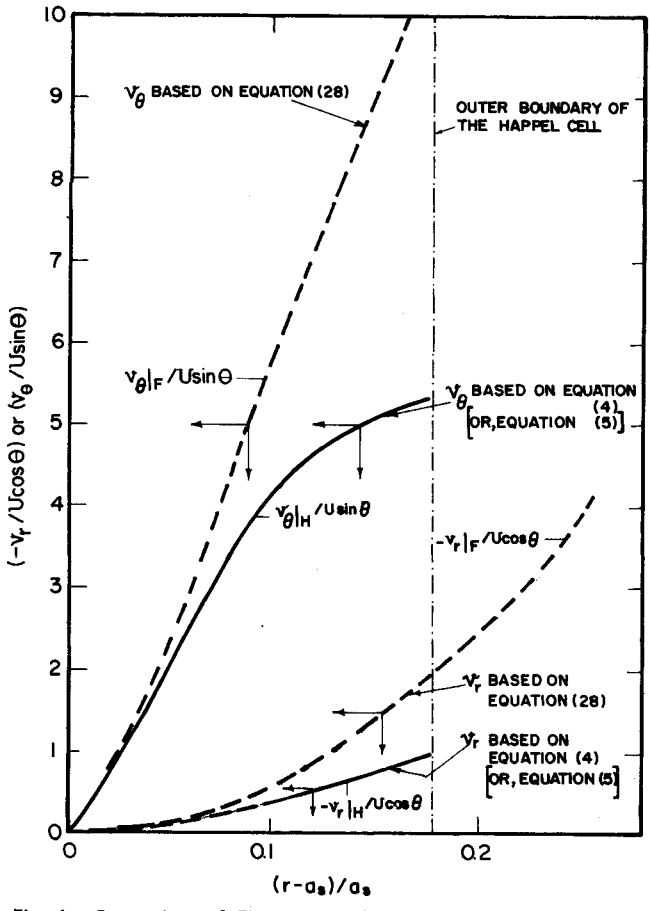

Fig. 6a. Comparison of Fitzpatrick's (1972) velocity field with that of Happel's model within the liquid shell.

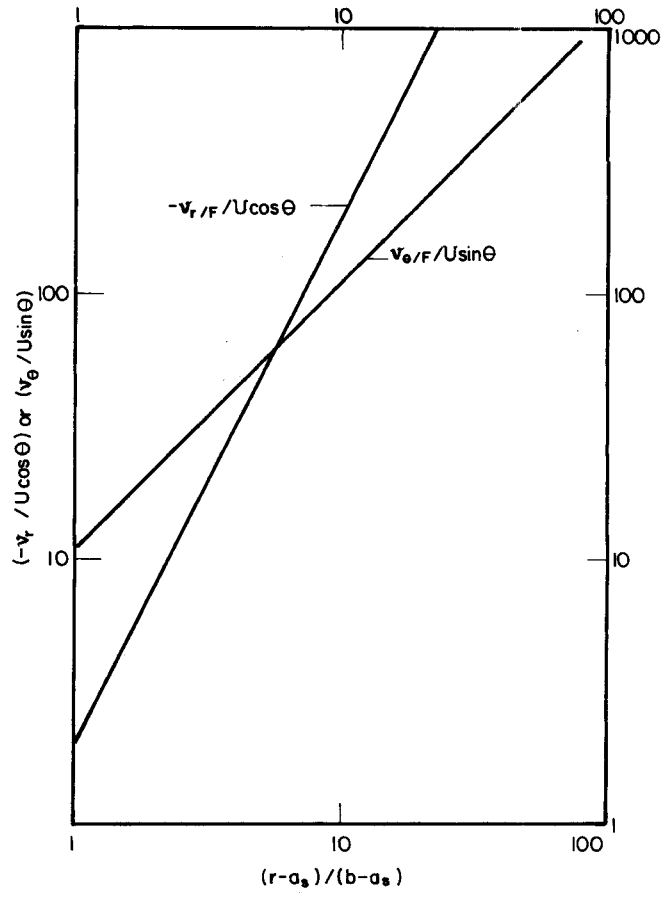

Fig. 6b. Fitzpatrick's velocity field outside the liquid shell as a function of shell thickness.

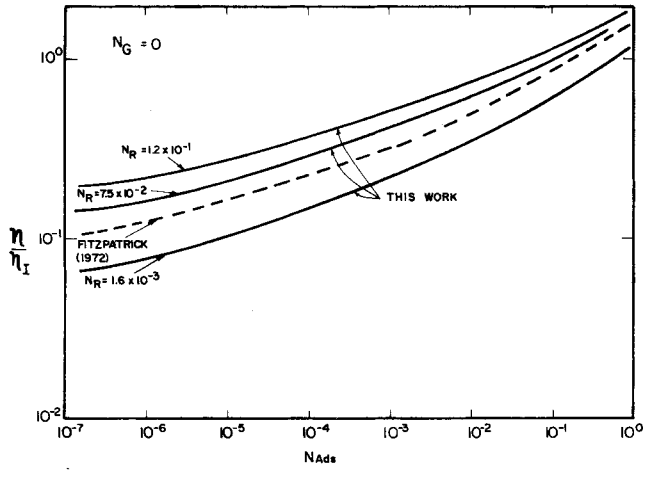

Fig. 7. Comparison of the theoretical predictions of this work with those of Fitzpatrick (1972).

21 μm, whereas the Happel shell is only about 18 μm thick. On the other hand, the termination point of the trajectory is about 100 a_p, which is equal to 1 050 μm ($\approx 6d_s$ or 60 times the shell thickness). Figure 6 clearly indicates the large deviation between the velocity profiles used by FitzPatrick and those corresponding to Happel's model when the point of termination is so far away.* Consequently, the results represented by their calculations are entirely different from those based on Happel's model.

The other approximations made by these investigators result in the elimination of one process parameter from the final correlation for η. Spielman and FitzPatrick present (η/η_I) as a function of $N_{Ad,s}$ and $N_{Gr,s}$. Although $N_{Ad,s}$ and $N_{Gr,s}$ are obtained as combinations of N_G, N_{Lo}, and N_R, their final results do not represent the effect of N_R on η completely. As an example, Figure 7 presents (η/η_I) vs. $N_{Ad,s}$ for various values of N_R (with $N_G = 0$; that is, $N_{Gr,s} = 0$). The results of FitzPatrick do not show dependence on N_R at constant $N_{Ad,s}$, whereas the present work does show that (η/η_I) varies by a factor of about 4 as N_R is varied and $N_{Ad,s}$ is held constant. (The range of N_R shown in Figure 7 corresponds to the upper and lower limits of N_R used in FitzPatrick's experiments.) The variation diminishes for high values of $N_{Ad,s}$. However, such high values of $N_{Ad,s}$ correspond to low values of d_p, and hence the contribution due to Brownian motion increases significantly. Therefore, the trajectory calculations have greater significance only for low values of $N_{Ad,s}$.

A comparison between the results of the present study and those based on the model of Payatakes et al. (1973*a* and *b*) is shown in Table 3. The results shown are for the experimental data presented by Ison and Ives (1969). The agreement between the theoretical calculations and the experimental data will be discussed in the following section. In the present section, we examine the corespondence between Happel's model and the constricted tube model. It is clear from Table 3 that in most cases the predictions of Happel's model are in close agreement with those of the constricted tube model. This is very much desirable since it is convenient to combine Happel's model and the constricted tube model in theoretical analyses of deep-bed filtration. As mentioned earlier, the Happel model is convenient for predicting collection rates (because of the availability of closed-form solution for the flow field), whereas the constricted tube model is more attractive for studying pressure drops (because of its geometric similar-

* The velocity profiles based on Equation (5), which are used in this work, coincide with those based on Equation (4) (see Figure 6).

TABLE 3. COMPARISON OF THE PRESENT WORK WITH THE EXPERIMENTAL DATA OF ISON AND IVES (1969)

$\lambda \times 10^2$, cm^{-1}

	$d_p = 2.75\ \mu$m			$d_p = 4.5\ \mu$m			$d_p = 9.0\ \mu$m		
Run No.	Expt'l data	Payatakes (1973)	This work*	Expt'l data	Payatakes (1973)	This work*	Expt'l data	Payatakes (1973)	This work*
I	6.0	2.4	2.4	7.6	3.2	3.4	8.8	7.1	9.6
II	8.1	3.1	2.6	11.0	4.6	3.9	14	10.5	10.4
III	11.0	4.1	2.7	15.0	6.2	4.1	16.5	14.2	10.4
IV	3.1	1.8	2.2	4.6	2.5	3.7	6.4	5.0	9.2
V	3.1	1.2	1.8	4.4	1.7	3.3	5.6	3.7	9.1
VI	4.5	2.1	1.5	5.8	3.3	2.2	6.3	7.7	6.0
VII	3.9	1.9	1.1	4.4	3.1	1.5	4.6	8.2	3.5
VIII	2.7	1.7	0.7	3.9	3.1	1	5.3	8.2	2.3

* The corresponding values based on Spielman and Fitzpatrick (1973) are given in Payatakes et al. (1974c) and are markedly higher, especially for large d_p (for example, for $d_p = 9\mu m$, they are about four to ten times higher than those based on the rigorous application of the sphere-in-cell model).

ity with the pore structure of the bed). Table 3 shows that such a combination is indeed reasonable.

COMPARISON WITH EXPERIMENTAL DATA

Equation (27) covers the range of powers of d_p, d_s, U, μ, etc., commonly observed in deep-bed filtration data. However, it is instructive to compare its predictions with some of the typical filtration data available in the literature. In Figures 8, 9, and 10 we have presented the theoretical values along with the experimental data of Fitz-Patrick (1972), Yao (1968), and Ghosh et al. (1975).

We have chosen to use the data of these investigators for the following reasons:

1. All of these investigators have used well-defined systems, such as uniform grains and particles.
2. The Hamaker's constant and other parameters necessary for computing the various dimensionless groups [including those that do not appear in Equation (27) such as the double-layer interaction groups] are clearly defined.
3. All these investigations cover (experimentally) all important mechanisms (that is, diffusion, interception, sedimentation, and surface forces including unfavorable double-layer repulsion).

It is clear from the above figures that the theoretical predictions based on the present work are indeed very close to the experimental observations. In fact, even the relative significance of the transport mechanisms is estimated well by the model. For example, Figure 8 shows the results of FitzPatrick's experimental data corresponding to $d_p = 21\ \mu$m. Because of the large size of the suspended particles in this case, the role of Brownian motion is insignificant, and it is confirmed by the theoretical results [based on Equations (22) and (26)]. On the other hand, for smaller particles one would expect a substantial amount of diffusion. Figure 9, which presents FitzPatrick's experimental data for $d_p = 1.3\ \mu$m, supports this expectation. As shown in the figure, exclusion of diffusion from the theoretical calculations [that is, use of Equation (26)] results in poorer agreement, thereby indicating the necessity of including the contribution due to diffusion. When the theoretical values are adjusted for collection due to diffusion, the agreement is clearly satisfactory.*

Additional evidence of the usefulness of this work can be seen in Figure 10, which covers the entire range of d_p usually encountered in water filtration. The data presented are from the works of Yao (1968) and Ghosh et al.

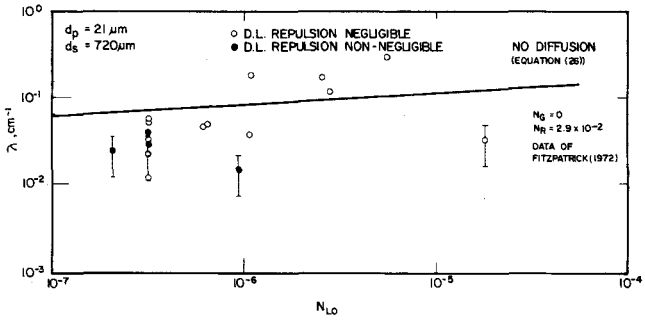

Fig. 8. Comparison with Fitzpatrick's experimental data (interception dominant).

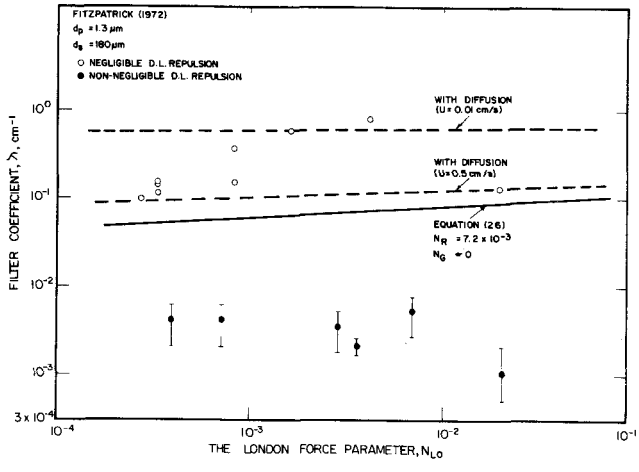

Fig. 9. Comparison with Fitzpatrick's experimental data (diffusion dominant).

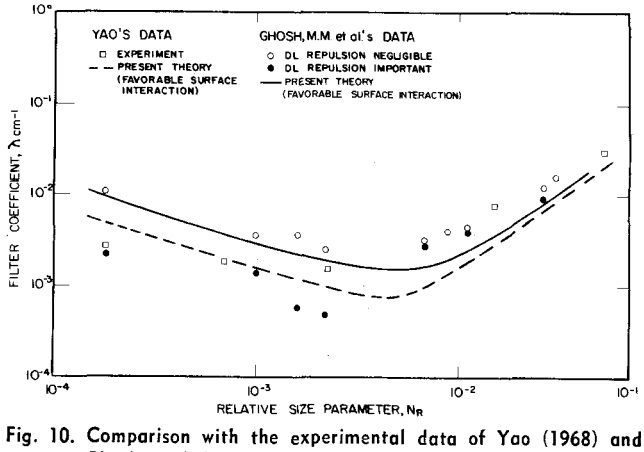

Fig. 10. Comparison with the experimental data of Yao (1968) and Ghosh et al. (1975). (All mechanisms are significant).

* Collection due to diffusion depends on the Peclet number. Since the experimental data presented in Figure 9 correspond to various values of N_{Pe}, we have shown the theoretical results corresponding to the upper and lower limits of the range covered by N_{Pe}.

(1975), and the major variable here is d_p. The agreement between the theoretical calculations and the experimental data is indeed more than one could expect, since the differences in all these cases are within the fluctuations of the experimental data under identical conditions. In fact, as shown in Table 3, the theory is reasonable even in the case of comparison with experiments where the parameters have not been controlled as closely as in the case of the above investigations.

CONCLUSION

The results above and the discussion that follows them clearly establish the usefulness of the present work under a variety of conditions. The model is accurate enough in the sedimentation-interception range as well as in the diffusion dominated region. To facilitate easier accessibility to this model, a closed-form expression [Equation (27)], which is sufficiently accurate, is also presented in this paper. Furthermore, the predictions of the present work parallel those of the constricted tube model proposed by Payatakes et al. (1973*a* and *b*), so that the present work can be used in place of the latter for calculating retention rates in deep-bed filters while retaining the constricted tube model for pressure drop estimations.

ACKNOWLEDGMENT

This work was performed under Grant No. GK-33976, sponsored by the National Science Foundation.

NOTATION

a_p = particle radius
a_s = collector radius (see Figure 1)
A = coefficient in Equation (5)
A^+ = dimensionless A defined by $A\,a_p^2/U$
A_s = $2(1 - p^5)/w$; defined in Equation (16)
b = radius of the Happel cell (see Figure 1)
B = coefficient in Equation (5)
B^+ = dimensionless B defined by $B\,a_p/U$
C_o = concentration of the particles is the suspension, number/unit volume
d_p = particle diameter
d_s = collector diameter
D = coefficient in Equation (5)
D^+ = dimensionless D defined by $D\,a_p^2/U$
D_{BM} = Brownian diffusion coefficient; see Equation (20)
$\mathbf{e}_r$, $\mathbf{e}_\theta$, $\mathbf{e}_\phi$ = unit vectors in r, θ, and ϕ directions
f_r^t, f_θ^t, f_r^m, $f^m{}_{1\theta}$, $f^m{}_{2\theta}$ and $f_\theta{}^r$ = drag correction factors in Table 1; functions of δ
$\mathbf{f}$ = force vector acting on the particle; superscript specifies the source of the force; for example, $\mathbf{f}^{DL}$ is the force due to double-layer interaction (see Table 1)
g = magnitude of the vector, $\mathbf{g}$
$g_\phi{}^r$, $g_\phi{}^t$, $g^m{}_{1\phi}$ and $g^m{}_{2\phi}$ = torque correction factors in Table 1; functions of δ
$\mathbf{g}$ = acceleration due to gravity
H = Hamaker constant ($\sim 1 \times 10^{-13}$ erg)
k = Boltzmann constant (1.38048×10^{-16} erg/°K)
K_1, K_2, K_3, K_4 and K_3' = coefficients that appear in Equations (1) and (2)
$N_{Ad,s}$ = adhesion group in FitzPatrick (1972); $N_{Ad,s} = N_{Lo}/(A_s N_R^2)$
N_{DL} = double-layer group; $D_{DL} = \kappa a_p$
N_{E1} = electrokinetic group #1; $N_{E1} = \nu\kappa(\zeta_c^2 + \zeta_p^2)/12\pi\mu U$
N_{E2} = electrokinetic group #2; $N_{E2} = 2\zeta_c\zeta_p/(\zeta_c^2 + \zeta_p^2)$
N_G = gravity group; $N_G = 2a_p^2(\rho_p - \rho_f)g/9\mu U$
$N_{Gr,s}$ = gravity group in FitzPatrick (1972); $N_{Gr,s} = N_G/(A_s N_R^2)$
N_{Lo} = London group; $N_{Lo} = H/9\pi\mu a_p^2 U$
N_{Pe} = Peclet number; $N_{Pe} = Ud_s/D_{BM}$
N_R = relative size group; $N_R = a_p/a_s$
N_{Rtd} = retardation group; $N_{Rtd} = 2\pi a_p/\lambda_e$
p = a_s/b, defined in Equation (1)
r = radial coordinate (see Figure 1)
r^+ = r/a_p
r^* = dimensionless radial coordinate, $r^* = r/a_s$
$r_o{}^+$ = r^+ corresponding to the start of integration of the trajectory equation
$r_s{}^+$ = termination point of the trajectory; $r_s{}^+ = b/a_p$
$\mathbf{r}$ = position vector; $\mathbf{r} = (r, \theta)$
$\mathbf{r}^*$ = dimensionless position vector; $\mathbf{r}^* = (r/a_s, \theta)$
$\mathbf{r}_o{}^+$ = $(r_o/a_p, \theta_o)$
$\mathbf{r}_s{}^+$ = $(r_s/a_p, \theta_s)$
s_1 = $(f_\theta{}^t g_\phi{}^r - f_\theta{}^r g_\phi{}^t)/g_\phi{}^r$
s_2 = $(f_\theta{}^r g^m{}_{1\phi} + y^+ f^m{}_{1\theta} g_\phi{}^r)/g_\phi{}^r$
s_3 = $(f_\theta{}^r g^m{}_{2\phi} + y^+ f^m{}_{2\theta} g_\phi{}^r)/g_\phi{}^r$
t = time variable
T = absolute temperature of suspension
$\mathbf{t}$ = torque vector acting on the particle; superscript specifies the source of the torque
$\mathbf{u}$ = particle velocity vector; subscript denotes the particular component
U = approach velocity of the liquid
$\mathbf{v}$ = liquid velocity field
w = function of (a_s/b) defined in Equation (1)
y = $(r - a_s)$, see Figure 1

Greek Letters

α = retardation correction; a function of δ, a_p, and λ_e (see Table 1)
δ = surface-to-surface separation between the collector and the particle (see Figure 1)
δ^+ = δ/a_p
ϵ = initial porosity of the filter bed
ζ_c = zeta potential of the collector
ζ_p = zeta potential of the particle
η = initial collection efficiency
η_G, η_I = collection efficiencies due to sedimentation and interception, respectively
θ = angular coordinate (see Figure 1)
θ_o = θ corresponding to the start of the integration
θ_s = θ corresponding to the termination of the integration (see Figure 1)
κ = Debye-Hückel reciprocal length
λ = filter coefficient
λ_e = wavelength of electron oscillation; $\lambda_e = 1\,000$ Å
μ = viscosity of suspension
π = 3.14159... rad
ρ_f = density of the liquid
ρ_p = density of the particle
ν = dielectric constant of the medium (~ 81)
ψ = stream function
ω = magnitude of the angular velocity of the particle
$\boldsymbol{\omega}$ = angular velocity of the particle

LITERATURE CITED

Brenner, H., "The Slow Motion of a Sphere through a Viscous Fluid Towards a Plane Surface," *Chem. Eng. Sci.*, **16**, 242 (1961).

Cookson, J. T., "Removal of Submicron Particles in Packed Beds," *Environ. Sci. Tech.*, 4, 128 (1970).

FitzPatrick, J. A., "Mechanisms of Particle Capture in Water Filtration," Ph.D. dissertation, Division of Engineering and Applied Physics, Harvard University, Cambridge, Mass. (1972).

Ghosh, M. M., T. A. Jordan, and R. L. Porter, "Physicochemical Approach to Water and Wastewater Filtration," *J. Environ. Eng. Div., Proc. ASCE*, EE1, 71 (1975).
Goldman, A. J., R. G. Cox, and H. Brenner, "Slow Viscous Motion of a Sphere Parallel to a Plane Wall: I. Motion through a Quiescent Fluid," *Chem. Eng. Sci.*, **22**, 637 (1967*a*).
———, "II. Couette Flow," *ibid.*, 653 (1967*b*).
Goren, S. L., and M. E. O'Neill, "On the Hydrodynamic Resistance to a Particle of a Dilute Suspension When in the Neighborhood of a Large Obstacle," *ibid.*, **26**, 325 (1971).
Happel, John, "Viscous Flow in Multiparticle Systems: Slow Motion of Fluids Relative to Beds of Spherical Particles," *AIChE J.*, **4**, 197 (1958).
Hogg, R., T. W. Healy, and D. W. Fuerstenau, "Mutual Coagulation of Colloidal Dispersions," *Trans, Faraday Soc.*, **62**, 1638 (1966).
Ison, C. R., and K. J. Ives, "Removal Mechanisms in Deep Bed Filtration," *Chem. Eng. Sci.*, **24**, 717 (1969).
Ives, K. J., "Filtration of Water and Wastewater," *Environ. Control*, **2**, 293 (1971).
O'Neill, M. E., "A Slow Motion of Viscous Liquid Caused by a Slowly Moving Solid Sphere," *Mathematika*, **11**, 67 (1964).
Payatakes, A. C., "A New Model for Granular Porous Media—Application to Filtration through Packed Beds," Ph.D. dissertation, Syracuse Univ., N.Y. (1973).
Payatakes, A. C., C. Tien, and R. M. Turian, "A New Model for Granular Porous Media: I. Model Formulation," *AIChE J.*, **19**, 58 (1973*a*).
———, "II. Numerical Solution of Steady State Incompressible Newtonian Flow through Periodically Constricted Tubes," *ibid.*, **19**, 67 (1973*b*).
Payatakes, A. C., R. Rajagopalan, and C. Tien, "Application of Porous Media Models to the Study of Deep Bed Filtration," *Can J. Chem. Eng.*, **52**, 722 (1974*a*).
Payatakes, A. C., C. Tien, and R. M. Turian, "Trajectory Calculation of Particle Deposition in Deep Bed Filtration: I. Model Formulation," *AIChE J.*, **20**, 889 (1974*b*).
———, "II. Case Study of the Effect of the Dimensionless Groups and Comparison with Experimental Data," *ibid.*, 900 (1974*c*).
Prieve, D. C., and E. Ruckenstein, "Effect of London Forces upon the Rate of Deposition of Brownian Particles," *ibid.*, 1178 (1974).
Rajagopalan, R., "Stochastic Modeling and Experimental Analysis of Particle Transport in Water Filtration," Ph.D. dissertation, Syracuse Univ., N. Y. (1974).
Spielman, L. A., and J. A. FitzPatrick, "Theory of Particle Collection under London and Gravity Forces," *J. Coll. Interface Sci.*, **42**, 607 (1973).
Weber, Jr., W. J., ed., *Physicochemical Processes for Water Quality Control*, Wiley Interscience, New York (1972).
Yao, K-M., "Influence of Suspended Particle Size on the Transport Aspect of Water Filtration," Ph.D. dissertation, Univ. N. C., Chapel Hill (1968).

Manuscript received November 21, 1975; revision received February 20, and accepted February 23, 1976.

Interfacial Phenomena in Falling Film Evaporation of Natural Seawater

The fluid dynamics and heat transfer of boiling seawater in falling film evaporators have been investigated. Large interfacial disturbances have been observed, caused by surfactants in seawater. Although these disturbances enhance heat transfer, they increase entrainment and the tendency for scale formation in fluted tubes.

VICTOR C. VAN DER MAST
and
LEROY A. BROMLEY

Department of Chemical Engineering and the Bodega Marine Laboratory
University of California
Berkeley, California 94720

SCOPE

Distillation of seawater in multiple effect falling film type of evaporators is an established technique to produce fresh water from seawater. In such evaporators, steam generated in one effect condenses on the outside of vertical tubes in the next effect, causing seawater inside the tubes to boil. The seawater runs down the inside tube wall in an annular type of flow. Because of the small temperature difference between the condensing steam and the boiling seawater, the boiling mechanism is generally one of evaporation at the liquid-vapor interface.

Substantial differences in heat transfer for natural seawater, sodium chloride solutions, and city water have been observed by other workers, but no conclusive explanations have as yet been given. These differences have sometimes been associated with the tendency of natural seawater to foam.

By using techniques developed specifically for this work, it was possible to measure inside heat transfer coefficients for localized areas, the waviness of the falling film, and the liquid entrained in the vapor phase. An approximate description of the morphology of the two-phase mixture inside the tube could thereby be obtained. This information provides insight into the heat transfer and fluid dynamic characteristics of falling film evaporation of natural seawater.

A new technology is emerging which uses fluted evaporator tubes instead of the usual smooth tubes. With respect to the inside of the tubes, the heat transfer and fluid dynamic characteristics have been previously investigated by others using mainly city water or sodium chloride solutions. This information may not be applicable for natural seawater, as shown in this paper.

Correspondence concerning this paper should be addressed to LeRoy A. Bromley.